# Towards the thermal utilisation of non-tyre rubbers – macroscopic and chemical changes while approaching the process temperature

Pal Szentannai[a,*], János Bozi[b], Emma Jakab[b], János Ősz[a], Tibor Szűcs[a]

[a] Budapest University of Technology and Economics, Department of Energy Engineering, Budapest, Hungary

[b] Hungarian Academy of Sciences, Research Centre for Natural Sciences, Institute of Materials and Environmental Chemistry, Budapest, Hungary

[*] Corresponding author. E-mail address: szentannai@energia.bme.hu (P. Szentannai)

***Abstract***

*This paper presents important changes in the basic fuel properties of non-tyre rubber wastes during heating from ambient to the temperature of the thermal conversion reactor. Experiments were carried out on both macroscopic and chemical processes occurring throughout the sample path. Special emphasis was put on the possible utilisation of non-tyre rubber wastes in Fluidised Bed Conversion units. The results show that some potential fuels studied may build sticky surfaces in the fuel feeding paths while all the samples undergo extensive fragmentation. Thermogravimetry/mass spectrometry experiments demonstrate that the volatile production occurs in two distinct temperature ranges characterised by the limits of about 150 – 350 °C and 350 – 550 °C. The gas chromatographic analysis shows that most of the chlorine- and nitrogen-containing compounds are formed in the first temperature range of pyrolysis and these products are released from the additives of the rubber samples. The duration of devolatilisation is 1.5 – 2.5 minutes under the normal fluidised bed combustion of 50 mm rubber particles. Considering the results achieved, the possible ways of practical applications is also formulated in this paper.*

***Keywords***

Waste Derived Fuel; Non-tyre rubber waste; Pyrolysis-GC/MS; TG/MS; FBC; Gasification

**Highlights**

- Non-tyre rubbers may build sticky surfaces at the temperature of the fuel feeding path.
- The extensive fragmentation starts at about 240 °C.
- The release of volatile products occurs in two distinct temperature ranges.
- Most of the chlorine- and nitrogen-containing compounds are released below 400 °C.
- The duration of the complete volatile release is several minutes under FBC conditions.

## 1. Introduction

Several sorts of waste rubber appear to be an attractive source for energy production because of their high calorific values, low or even negative prices, as well as legislative, financial, and environmental problems at conventional disposal [1–3]. The three main groups of available technologies are pyrolysis, gasification, and combustion.

Combustion seems to be the most widespread technology, which is characterised by the longest history, the high number of running commercial plants (see e.g. [4–6]) and its intensive research background [2,7–10]. Fluidised Bed Combustion (FBC) appears to be a very successful solution among the combustion methods for its well-known flexibility against fuel quality, being a beneficial property when using waste rubbers of rather variable compositions. It is interesting to mention a worldwide boom of building FBC plants firing waste rubber. One of the leading countries in FBC technology is Japan, where between 2005 and 2010 nine FBC plants were put into operation firing waste rubber [11].

Pyrolysis is another rapidly developing technique for the thermal utilisation of waste rubber, although the pyrolysis research started later than the studies on rubber combustion [12–15]. An up-to-date summary about pyrolysis [3] discusses its technical basics, industrial units, main development directions as well as its legislative and policy background.

Even though gasification is well-known and widely applied for various solid fuels for several decades, its application for rubber waste seems to be a quite new idea. Nevertheless, recent theoretical and experimental results on different kinds of waste rubber show that gasification is a promising method as well [15,16].

In all the above mentioned thermochemical conversion methods, a common and first event is the warming up of the fuel as it is evident that it has to be transported from the storage area into the reaction chamber. It is important to study the processes occurring in the fuel during transportation from the storage area to the feeding point since the temperature difference between these two endpoints is several hundreds of degrees Celsius and the fuel goes through the pipeline within a few tens of minutes.

The goal of the experimental investigation summarised in this paper was to gather information on the above topics applying the most relevant types of non-tyre waste rubber as a solid fuel. It was also considered that the physical and chemical processes occur dominantly in the feeding route at ambient pressure and gas composition while the last processes take place inside the reactor characterised by significantly elevated temperature, different atmosphere, and other conditions.

The phrase *rubber* covers an extremely wide range of materials described by various compositions, physical, and chemical properties [17,18]. Industrial rubber products are usually composed of 10 or more ingredients [17] and the main component is called *elastomer*. The repeating elements of these polymers

are called *monomers*, the selection of which basically determines the properties of rubber. Therefore, the rubbers are grouped by the elastomers (i.e., monomers). A list containing 27 common elastomers, together with their ASTM (American Society for Testing and Materials) designations can be found in the work cited above [17]. The most important and most frequently applied additive is carbon black and a large variety of further additives (e.g., plasticisers, antioxidants, fire retardants) is used as well [17].

An evident way of categorising waste rubber fuels could be based on the types of elastomers and other chemical components. In practical applications, this approach cannot be used because of the unknown chemical compositions of the individual waste particles. Therefore, another approach is used in the waste industry, which is based on the origin of the rubber wastes. Some relations between these two categorising approaches exist, however, a strict correspondence between them cannot be formulated. In the present paper the later categorising aspect is followed as this approach allows the possible application of the results to be presented here.

Rubber wastes are often categorised into two major groups of *tyres* and *non-tyre* products [19], both of which can be further subdivided. The current study focuses on two, industrially relevant subgroups of *non-tyre* products, namely hoses and manufacturing sprues. They were chosen as a result of previous feasibility studies with special emphasis on their qualities, amounts and predictable availabilities.

Although waste tyres were excluded from this study, the published literature and experience on the applications were carefully studied and considered. Tyres, especially those of private cars, motorbikes, and small lorries are mainly made of styrene-butadiene rubber (SBR) [19], however, the quality and amount of additives still allow a high variety within this widely investigated group.

It is interesting to note that the main problem of tyre utilisation for power generation seems to be the presence and removal of wires [4–6]. In addition to a few unusual solutions [20,21], most of the technical papers report about 94 – 95% success rate in removing wires from various locations of the fluidised bed boilers [6]. It is also important to mention that milling or cutting rubber waste, even after a proper wire removal, is difficult and energy intensive. This makes FBC even more advantageous because of its particle size flexibility.

The scientific papers on the thermochemical conversion of tyres report some interesting findings, which may be important for non-tyre fuels as well. The phenomenon of primary fragmentation was described by a research group [9,22], which seems to be the characteristic of all sorts of rubber. This process has very high importance in the fluidised bed conversion technique. The same group also gives a theoretical description of tyre pyrolysis, which was divided into three phases [2,23]. It was verified by measurements of the weight losses while heating up the tyre particles.

Another research group measured the hydrodynamic characteristics of combusting tyre in an FBC and the mass loss of tyre was monitored during heating up [10]. It was observed that pyrolysis of the tyre occurs in two stages but the composition of the evolved products in the two stages were not detected. Dynamic thermogravimetric investigations were carried out on rather big samples (about 30 g) of SBR [14] and the yield of gas, tar, and char components were measured under various pyrolysis conditions. A strong influence of the heating rate and the oxygen concentration was shown in an earlier publication [24]. The differential thermogravimetric (DTG) curves showed a double-peak character, which was not further investigated at that time.

Non-tyre waste rubbers as a promising resource for thermal utilisation were investigated at a lower intensity than tyres. Important data and observations were reported on the combustion behaviour and the pollutant emission during firing nitrile-butadiene rubber (NBR) balls and woodblocks in an FBC reactor [16,25,26]. FBC technology was used [12] for a non-tyre chloroprene rubber (CR) which has a high annual production in Germany. Gas chromatographic (GC) analysis was carried out focusing on the chlorinated aromatic compounds in the volatile products. The final temperature of the reactor was 593 °C, and the important GC results obtained refer to this single temperature. The total amount of syngas was measured [15] during pyrolysis and gasification of butadiene rubber (BR) at higher temperatures (800 °C and 900 °C). An important observation was that the duration of rubber gasification was several minutes under these conditions.

It is a generally known macroscopic behaviour of rubber that the pieces fall apart into powder-like, very small particles during heating, which is called primary fragmentation. Another intermediate macroscopic change may occur, however, it is very rarely mentioned. Some rubber materials have the tendency for getting sticky, which is essentially important for the design of fuel feeding routes. The only source found where this behaviour is described calls this phenomenon as “sticky combustion surface” [27].

## 2. Materials and methods

### *2.1. Test materials*

The non-tyre rubber samples were taken from waste management enterprises, which appear to be long-term suppliers of a commercial power plant in Hungary. The suppliers' rules and methods of waste rubber classification were adopted and followed.

Two subgroups of *non-tyre* rubber wastes were selected in a preliminary study because of their permanent availabilities and approximately equal qualities. Both of them are production scraps, which assures their relative cleanness without much unpredictable external pollutions.

The term hose refers to the first type of non-tyre rubber wastes investigated and discussed in this paper. Hoses are produced from a wide range of elastomers but butadiene is one of the most important

monomers constituting butadiene rubber and nitrile butadiene rubber [17,19]. The investigated samples originated most probably from car industry. However, their diameters and appearance varied considerably and their constructions also had various elements. Hoses contained (see Fig. 1a) several layers of the rubber body, a braided fibre reinforcement mesh, and an inner liner. Some of the samples had an external polymer net. The samples were cut into pieces of about 50 mm on the waste management site and this process made the mesh of the reinforcement fibre visible and fuzzy. The laboratory analysis of hoses shows (Table 1) that the heating value is in the range of the best quality coals (32 MJ/kg) and it is a highly volatile (47.4%) solid fuel, having low moisture content (0.6%).

Manufacturing sprue, sprue in the following, is the term referring to the second type of non-tyre rubber wastes discussed in this paper. More precisely, the test materials referred to as sprues include all the parts remaining as scraps after injection moulding, not just the strictly conceived sprues, but also mould runners and gates. In contrast to the hoses, sprues appear to be homogeneous but their shapes and sizes are rather different (see Fig. 1b). The sprue samples remained from the moulding process of rather elastic elements like seals. Seals are used in a number of applications where conformity to irregular surfaces is required.

*2.2. Single particle heater*

An electrically heated oven was used for observing the behaviour of the single fuel particle during heating (Fig. 2). The internal temperature of the oven can be programmed up to 1200 °C applying a controlled heating rate. The internal surface of the oven is covered with refractory concrete insertion and there are two heaters on the sidewalls. The internal dimensions of the heated volume are 445 mm x 170 mm x 131 mm (LxWxH). A rod was used in order to keep the sample at a stable position. This rod can be used with two kinds of heads: a spoon and a lance. The spoon is designed to hold small and numerous pieces while the lance is for bigger samples that can be stuck up. The sample on the head of the rod was pushed into the oven. The door was kept open to allow natural air flow and visual observation. During the heating procedure, the internal temperature of the sample was continuously measured and the visual information was also digitally recorded.

In the experiments, a small sample of about 8–10 g was put into the cold oven in a stagnant air atmosphere, which was observed during the heating in steps of 50 °C. The heating rate was set to the highest possible value (1 °C per 3 seconds). It was possible to pull out the sample during the experiment to examine it more precisely.

*2.3. Thermogravimetry/mass spectrometry (TG/MS)*

Prior to the analytical measurements, representative pieces of the samples were cryomilled to fine powder in an MM 301 type mixer mill (Retsch GmbH, Germany). The powdered samples of hoses and

sprues were analysed by TG/MS. The TG/MS measurements were performed using a modified Perkin-Elmer TGS-2 thermobalance coupled to a Hiden HAL 2/301 PIC mass spectrometer using a glass-lined metal capillary heated at 300 °C. Approximately 1 mg sample was placed into the platinum sample holder of the thermobalance. Before the experiments, the apparatus was purged for one hour with the argon carrier gas at a flow rate of 140 mL $min^{-1}$. The samples were heated at a 40 °C $min^{-1}$ rate up to 1000 °C in the argon atmosphere. The volatile products were analysed online by the quadrupole mass spectrometer, which was operated at a 70 eV electron energy. The ion intensities were normalised to the sample mass and to the intensity of the $^{38}Ar$ isotope of the carrier gas.

*2.4. Pyrolysis-gas chromatography/mass spectrometry (Py-GC/MS)*

Py-GC/MS experiments were performed in a Pyroprobe 2000 pyrolyser (Chemical Data Systems, Inc., USA) interfaced to a gas chromatograph/mass spectrometer (Agilent 6890/5973). Approximately 1 mg cryomilled sample was placed into a quartz tube sample holder. This tube was put into the platinum coil of the pyrolyser probe. The probe was inserted into the pyrolysis chamber, which was held at 280 °C in order to avoid the condensation of pyrolysis products. The chamber was purged with helium carrier gas for 1 minute, then the sample was heated to 550 °C, and held there for 20 seconds. The helium carrier gas at a flow rate of 20 mL $min^{-1}$ purged the volatile products from the pyrolysis chamber to the GC. The GC analysis was performed using a DB-1701 type capillary column (30m×0.25mm×0.25μm, Agilent Technologies, USA). A single ramp temperature program was applied for the separation of the pyrolysis products. After an isothermal period at 40 °C for 4 minutes, the GC oven temperature was programmed at a 10 °C $min^{-1}$ heating rate to 280 °C and held at the final temperature for 15 minutes. The separated pyrolysis products were detected by the MS operating in an electron impact mode (EI) at a 70 eV electron energy. The spectra were scanned over a mass range of 14-500 Da. The GC/MS identification of the pyrolysis products was carried out by using NIST mass spectral library, mass spectrometric identification principles and gas chromatographic retention relations.

Successive pyrolysis experiments were carried out at two temperature steps. The pyrolysis temperature was set to 350 and 300 °C for the hoses and sprues, respectively. After the first pyrolysis experiment, the sample was further pyrolysed at 550 °C. All the other pyrolysis and GC/MS parameters were the same as described above.

*2.5. Bubbling Fluidised Bed Combustor (BFBC)*

A mid-scale FBC test rig was used, which was set to bubbling mode. The basic configuration and the relevant measurement points of the apparatus are shown in Fig. 3. The height of the cylindrical combustion chamber is 5.00 m, its internal diameter is 158 mm. It has an internal refractory concrete insertion. The primary air enters through 30 nozzles to ensure a homogeneous distribution. The secondary

and tertiary air flows pass through simple pipes in the heights of 1300 and 1900 mm, respectively. The fuel enters above the nozzles through the feeder pipe. There is a gas burner above the nozzles to preheat the chamber and to support the combustion. The apparatus is equipped with a lot of measurement points, the relevant ones are shown in Fig. 3.

## 3. Results and discussion

### *3.1. Primary fragmentation*

Primary fragmentation while heating up seems to be a common property of rubber derived fuels although mainly tyres were studied [2,9,22,23]. The fragmentation is a critical phenomenon during transportation and utilisation in fluidised bed combustors. Therefore, the primary fragmentation was also studied on the actual non-tyre test materials.

Both non-tyre samples showed the characteristics of primary fragmentation. Upon the devolatilisation (from about 240 °C), the rubber body of the hoses and the entire sprues lost their flexibilities. They became fragile and fell apart into fine particles under a minimal mechanical agitation, very similarly to the behaviour of tyre observed several times [9,22]. The time scale of this fragmentation is definitely driven by the heating rate alone. The particle size of the fragments ranges from 1 μm up to 200 μm. There was no significant difference between hoses and sprues in this regard. Figure 4 shows a fragmented hose after reaching the temperature of 240 °C.

The primary fragmentation requires special attention during fluidised bed combustion as the fine fragments are lighter than the average particles of the bed, hence they are expected to leave the bed or even the freeboard before the complete burnout. This leads to potential energy loss or even environmental problems. Therefore, the residence time of these fragments has to be considered during the design of the boiler.

### *3.2. Building sticky surfaces*

Another interesting and important phenomenon was observed in a few sprue samples during the heating up procedure in the single particle heater. A few pieces of sprue samples (nearly 10%) started to melt and to be sticky at about 200 °C and this phenomenon ended at the initial temperature of devolatilisation and fragmentation at about 240 °C. The stickiness of the particles was observed visually and mechanically by touching them with a steel wire at each step of the observation temperatures. This behaviour has rather high practical significance since it might cause problems in the relatively hot parts of the feeding system. The reasons for this behaviour and especially the reasons for getting some sprues sticky and others not, need further studies.

During the later phases of the heating procedure, these melted samples acted similarly to the others, this is the reason why they started to be fragile as well. At the end of the process, there was not any

difference between the regular and the melted samples, which means that this behaviour did not affect the thermochemical reaction itself.

Another notable component of the sticky characteristic feature is the internal film layer of the hoses. It is less important than the stickiness of sprue surface because it is completely inside the tubes. Therefore, the hose cannot stick practically to anything during the thermal conversion process.

*3.3. Evolved gas components – TG/MS-analysis*

During combustion, the devolatilisation of the materials represents the first process followed by the combustion of volatile products in the vapour phase. Henceforth, we studied the release of the volatile products in an inert atmosphere in order to identify the individual compounds. Furthermore, the volatile decomposition products provide information about the composition of the rubber samples including the type of elastomer components and the nature of additive materials.

Figure 5 shows the (TG) and (DTG) curves of hoses. The thermal decomposition of hoses takes place in two distinct temperature ranges at 150-390 °C and 390-540 °C with mass losses of 29% and 30%, respectively (Table 2). Additionally, 3% mass loss occurs between 540 and 1000 °C that can be attributed to the final charring process of the polymeric constituents of rubber. Thus, the amount of the remaining solid residue is about 38% of the initial sample mass.

The MS analysis of the volatile compounds revealed that the mass loss in the first decomposition range (150-390 °C) is due to the elimination of $H_2O$, $SO_2$, and aliphatic products (see ion curves of *m/z* 18, *m/z* 64, and aliphatic fragments in Fig. 6a). Both saturated (*m/z* 43) and unsaturated (*m/z* 69) aliphatic fragment ions were detected. It can be supposed that products of high molecular mass are also released at this temperature range, which have been analysed in detail by Py-GC/MS measurements, discussed in Section 3.4. Figure 6b shows the evolution profiles of a few characteristic fragments and molecular ions forming between 390 and 540 °C from the hoses. The molecular ions of butadiene and isoprene indicate that the elastomeric components of the sample decompose to monomers at the second stage of pyrolysis. Furthermore, isobutene (or butene) is also produced during pyrolysis. Since the aliphatic decomposition products are strongly fragmented in the MS, we can detect several fragment ions in addition to the molecular ions. For instance, *m/z* 67 and *m/z* 41 ions seen in Fig. 6b are representative fragments of isoprene and isobutene (butene), respectively.

The TG and DTG curves of sprue sample are shown in Fig. 7. Its thermal decomposition also takes place in two stages similarly to the hose sample. However, there are some characteristic differences in the thermal properties and the products. The sprue sample starts to decompose at 130 °C and the mass loss is only 13% up to 310 °C. The decomposition in the first stage occurs at a much lower temperature than that of the hose sample (Table 2). In the temperature range of 310-530 °C, the formation of volatile

products results in 50% mass loss, i.e., the main devolatilisation of the major components of rubber takes place in this range. The charring process produces only 2% volatile products above 530 °C leaving little more than 34% solid residue.

In the first decomposition stage (130-310 °C) we could not detect any pyrolysis products by TG/MS, probably due to condensation in the transfer line. Fast pyrolysis experiments were applied to study these products, which is demonstrated later. Figure 8 illustrates the most significant ion profiles forming in the second stage of decomposition. The evolution curve of the molecular ion of butadiene (*m/z* 54) shows that it is released from two or three sources (e.g., different copolymers) resulting in multiple evolution peaks between 340 and 530°C. The evolution profiles of the molecular and fragment ions of isoprene (*m/z* 68 and 67) indicate multiple origins, however, the majority of this monomer is formed between 410 and 530°C. As Fig. 8 shows the intensity of the *m/z* 53 ion is the highest among the selected ions. It represents the molecular ion of acrylonitrile and the fragment ions of several unsaturated aliphatic products, including butadiene and isoprene. Aromatic hydrocarbons (e.g., benzene, toluene and xylenes) can also be detected, which probably originate from styrene copolymers. A characteristic aromatic fragment ion, *m/z* 91 is presented in Fig. 8. The evolved products of the second decomposition stage are presumably derived from polymers or various copolymers of butadiene, isoprene, styrene, and acrylonitrile.

*3.4. Evolved gas components – Py-GC/MS analysis*

The volatile products were also studied by fast pyrolysis, which is a suitable method for the analysis of the higher molecular mass compounds. The Py-GC/MS experiment of the hose sample at 550 °C resulted in the pyrolysis chromatogram, known as pyrogram, shown in Fig. 9a. The identification of the most important chromatographic peaks can be found in Table 3, which shows that a wide range of pyrolysis products can be detected including unsaturated aliphatic and alicyclic compounds as well as aromatic hydrocarbons, chlorinated alkanes, alcohols, and ester compounds. The relative intensities of the pyrolysis products were also calculated and presented in Table 3. It must be mentioned that only those products were taken into consideration which had a relative intensity above 1% of the total amount of the products. The sensitivity of the MS varies depending on the type of the compounds. However, the intensity of the individual products can be compared among the different pyrolysis experiments (e.g., normal and successive pyrolysis) since the peak areas were normalised to the sample sizes.

The main pyrolysis products of the elastomer compounds of the hose sample are butadiene and isoprene. The formation of styrene and other substituted benzenes indicates that styrene is a constituent of the rubber, for example in the form of styrene-butadiene rubber as well. Furthermore, the release of isobutene points to the presence of isobutene among the constituting monomers of the rubber copolymers (e.g., butyl rubber). The unsaturated cyclic compounds are also derived from the elastomer polymers.

Besides the usual rubber monomeric products, chlorinated alkanes, alcohols, esters, and n-alkanes were detected during the pyrolysis of hoses at 550 °C. It is supposed that these decomposition products can be attributed to various additives present in the rubber. The results of the TG/MS experiment showed a two-stage decomposition pattern, indicating that the evaporation of the additives occurs at a lower temperature than the decomposition of the polymeric components. In order to identify the additives, we carried out a two-stage pyrolysis experiment. On the basis of TG/MS experiments, at first the sample was heated to 350°C, which was a high enough temperature for the evaporation of most of the volatile additives. After the GC analysis of the products, we heated the residual sample further to 550°C. With this successive pyrolysis, the volatile additives could be distinguished from the decomposition products of the rubber polymers. Figure 9b and Table 3 demonstrate that several groups of products are released during the low temperature heating and their intensity is negligible or low at the second stage, indicating that they evaporated from the sample at 350°C. Chlorinated alkanes with carbon numbers $C_7$, $C_8$, and $C_9$ were apparently used as fire retardants and plasticisers. The cleavage of some functional groups occurs at relatively low temperature as the evolution of hydrogen-chloride and sulphur-dioxide indicates. The release of HCl can be explained by the scission of chlorine from the fire retardants. Sulphur dioxide can be formed from sulfonate side groups of certain additives. A few n-alkanes of high molecular mass were released from the hoses with carbon numbers $C_{26}$-$C_{29}$. Paraffin waxes are mainly used as lubricants during the extrusion process.

Trialkyl esters of aromatic acids are used as plasticisers in rubbers. Three alkyl esters of 1,2,4-benzenetricarboxylic acid 1,2,-anhydride with heptyl, octyl, and nonyl groups (peak #27, 29, and 31 in Fig. 9b and Table 3) were identified, which seem to be the most abundant additives of this sample. Apparently, the trialkyl ester compounds partially decompose at 350 °C resulting in the pyrolysis products of monoalkyl esters as well as 1-heptanol (peak #17), 1-octanol (peak #21), and 1-nonanol (peak #24). Figure 9c clearly shows that the decomposition of elastomer components takes place in the second step of the successive pyrolysis at 550 °C and only small amounts of additives remained for this stage of pyrolysis.

The pyrolysis of the braided fibre reinforcement was also studied. There was no detectable organic pyrolysis product of the fibre, indicating that the reinforcement is made of inorganic material (supposedly glass fibre).

The pyrolysis products of sprue sample forming at 550 °C clearly show that the sprues have different chemical composition than that of the hoses. As it can be seen in Table 4, a wide range of aliphatic and aromatic hydrocarbons and several nitrogen- and oxygen-containing organic compounds were identified. The relatively high yield of butadiene (peak #2 in Fig. 10) among the pyrolysis products indicates that butadiene represents the major monomer component of this elastomer. A cyclic dimer product of butadiene

polymers, 4-vinylcyclohexene (peak #8) is also released in relatively high intensity. Nevertheless, isoprene, styrene, acrylonitrile, isobutene, and compounds related to these pyrolysis products show evidence that the test material is a multi-component elastomer, such as poly(butadiene-styrene), poly(butadiene-acrylonitrile), and butyl rubber (isoprene isobutene copolymer).

The pyrogram of sprues also contains several peaks identified as polymer additives. Successive pyrolysis was applied to separate these additives from the pyrolysis products. As the TG data (Table 2) proved, the yield of these additives is much lower (13%) than that of the hoses (29%). Nevertheless, the MS sensitivity of these additives is very high, resulting in very intense peaks in the pyrograms. The pyrogram of sprues at 300 °C (Fig. 10b) clearly shows that the volatile additives evaporate and decompose at low temperatures (peaks #29, 31-37). As Fig. 10a and b along with Table 4 show, the most abundant product is tri(ethylene glycol) bis(2-ethylhexanoate) (peak #35), which is a widely used plasticiser. Several nitrogen-containing compounds can also be found in the pyrolysis oil. Nitriles are applied as plasticisers while aromatic diamines and quinoline derivatives are effective antioxidants. Aliphatic amides (e.g. # 33, 34) are used as antistatic agents, dispersion, and mould release agents. The additives of high molecular mass partially decompose during pyrolysis. Thus, there are some products in the pyrolysis oil which are apparently derived from the additives, e.g., peak # 25, 30 are decomposition products of peak #35. In the second stage of successive pyrolysis (Fig. 10c) the thermal decomposition of the polymer segments takes place primarily, nevertheless small amount of the residual additives can also be found in the pyrolysis oil.

*3.5. Duration of devolatilisation*

The time demand of devolatilisation of the waste derived fuel candidates was studied under the conditions existing generally inside a Fluidised Bed Combustor. Before the experiment, the combustion chamber was heated up to 850 °C and the velocity of the primary air was set to 3 m/s. There was about 5 kg of sand (0.1–0.7 mm diameter) in the chamber. Particles of typical size (about 50 mm long hoses) were dropped through the feeder into the preheated (850 °C) combustion chamber where the volatiles instantly started to be released and ignite. The duration of this process could be easily determined measuring the CO concentration of the flue gas. Figure 11 shows the CO concentration during the experiment of three samples. The duration of the peaks were 1.5–2.5 minutes, which gives very important information about the time demand of devolatilization under typical FBC conditions. A similar experiment was not performed on sprues because of their tendencies for sticking on the feeder tube and their rather irregular shapes and sizes.

## 4 Conclusions

The chemical composition of the two rubber samples slightly differs in the types of monomers and completely differs in the composition of the additives. The major monomers of hoses are butadiene, isoprene, styrene, and isobutene while butadiene, isoprene, styrene, and acrylonitrile represent the main monomers of the sprues. Hoses contain about 29 m/m % volatile additives including chloroalkane fire retardants and plasticisers, alkyl aromatic ester plasticisers, and n-alkane lubricants. Sprues release about 13 m/m % volatile additives, mostly tri(ethylene glycol) ester plasticiser and various nitrogen-containing compounds used as antioxidants and plasticisers.

The objective of the current work was to get a general overview about the physical and chemical changes non-tyre rubber fuels undergo on their ways from the storage areas to the reactor chambers of energy generation plants. Throughout this way, the fuel particles are significantly affected by temperature increase in addition to the mechanical influences. The devolatilisation of the non-tyre rubber samples occurs in two main stages during their heating up. The first stage begins at 130-150 °C with the evolution of the additives. It means that the release of volatiles may start within the feeding system of a fluidised bed combustor or within another reactor. The decomposition of the elastomer components occurs above 300-350 °C. Some pieces of the sprue samples start melting and build sticky surfaces before devolatilisation. The well-known primary fragmentation takes place in all the non-tyre rubber samples.

Some of the consequences of these effects require special considerations in the fuel feeder design and probably in the fuel selection. The low temperature devolatilization phase can be utilised if the volatile products (e.g., nitrogen and chlorine-containing additives) are suctioned at the appropriate places of the fuel feeding system. From the energetic point of view, a fuel feeder design would be optimal where the fuel does not warm up to the initial decomposition temperature and the residence time is significantly lowered.

If the amount of the sprues building sticky surfaces at a rather low temperature is significant, the blocking of some parts of the feeding system cannot be avoided. Further studies are required in order to determine the details and the reasons of this phenomenon using the single particle heating experiments.

## Acknowledgments

The research was initiated, financed, and permanently consulted by MVM Vértes Power Plant Ltd. and it is gratefully acknowledged. The participation of J. Bozi in this study was supported by the Hungarian National Research Fund (OTKA No. K83770) and by the “MTA Postdoctoral Fellowship Programme in Hungary”.

## References

[1] Anthony EJ. Fluidized bed combustion of alternative solid fuels; status, successes and problems of the technology. Prog Energy Combust Sci 1995;21:239–68. doi:10.1016/0360-1285(95)00005-3.

[2] Cammarota, A., Chirone, R., Salatino, P., Scala, F., Senneca, O. Fluidized Bed Combustion of Tyre Derived Fuel. Recycl. Reuse Used Tyres Proc. Int. Symp. Organised Concr. Technol. Unit Univ. Dundee, London: Thomas Telford; 2001.
[3] Antoniou N, Zabaniotou A. Features of an efficient and environmentally attractive used tyres pyrolysis with energy and material recovery. Renew Sustain Energy Rev 2013;20:539–58. doi:10.1016/j.rser.2012.12.005.
[4] Lundqvist, R. G. Fluidized bed combustion of unconventional fuels A few studies 2000.
[5] Kraft, D. L. Fluidized Bed Combustion of Tires 1994.
[6] Terasawa, Y., Shirahata, T., Takahashi, E., Nagatomi, M., Yokoshiki, T., Yamazaki, R. Operation Results of High-Temperature and -Pressure Fluidized Bed with Recycled Waste Fuels. Mitsubishi Heavy Industries, Ltd Technical Review 2005;42.
[7] Kim JR, Lee JS, Kim SD. Combustion characteristics of shredded waste tires in a fluidized bed combustor. Energy 1994;19:845–54. doi:10.1016/0360-5442(94)90037-X.
[8] Teng, Chyang, Shang, Ho. Characterization of Waste Tire Incineration in a Prototype Vortexing Fluidized Bed Combustor. Journal of the Air & Waste Management Association 1997;47:49–57.
[9] Scala F, Chirone R, Salatino P. Fluidized bed combustion of tyre derived fuel. Exp Therm Fluid Sci 2003;27:465–71. doi:10.1016/S0894-1777(02)00249-2.
[10] Holikova, K., Jelemensky, L., Annus, J., Markos, J. Investigation of tyres and coal combustion in a laboratory scale fluidized bed combustor. Petroleum and Coal 2005;47:10–25.
[11] Leckner, Bo (Ed.). Developments in Fluidized Bed Conversion During 2005-2010. A summary from the member countries of the IEA-FBC Implementing Agreement 2011.
[12] Kaminsky W, Mennerich C, Andersson JT, Götting S. Pyrolysis of polychloroprene rubber in a fluidised-bed reactor — product composition with focus on chlorinated aromatic compounds. Polym Degrad Stab 2001;71:39–51. doi:10.1016/S0141-3910(00)00147-6.
[13] Korenova, Z., Juma, M., Holíkova, K., Jelemensky, L., Markos, J. Experimental Study of Waste Rubber Pyrolysis and Combustion. Petroleum and Coal 2005;47:1–9.
[14] Grieco E, Bernardi M, Baldi G. Styrene–butadiene rubber pyrolysis: Products, kinetics, modelling. J Anal Appl Pyrolysis 2008;82:304–11. doi:10.1016/j.jaap.2008.05.004.
[15] Ahmed I, Gupta AK. Characteristic of hydrogen and syngas evolution from gasification and pyrolysis of rubber. Int J Hydrog Energy 2011;36:4340–7. doi:10.1016/j.ijhydene.2010.12.131.
[16] Kaewluan S, Pipatmanomai S. Gasification of high moisture rubber woodchip with rubber waste in a bubbling fluidized bed. Fuel Process Technol 2011;92:671–7. doi:10.1016/j.fuproc.2010.11.026.
[17] Schaefer RJ. Chapter 33: Mechanical Properties of Rubber. Shock Vib. Handb., McGraw-Hill; 2009.
[18] Erman B, Mark JE, Roland. The science and technology of rubber, fourth edition. Waltham, Mass.: Academic Press; 2013.
[19] De SK, White JR. Rubber Technologist’s Handbook. iSmithers Rapra Publishing; 2001.
[20] Sowards NK, Murphy ML. United States Patent: 5060584 - Fluidized bed combustion. 5060584, 1991.
[21] Sowards NK, Murphy ML. United States Patent: 5101742 - Fluidized bed combustion. 5101742, 1992.
[22] Arena U, Chirone R, Salatino P. The fate of fixed carbon during the fluidized-bed combustion of a coal and two waste-derived fuels. Symp Int Combust 1996;26:3243–51. doi:10.1016/S0082-0784(96)80170-6.
[23] Senneca O, Salatino P, Chirone R. A fast heating-rate thermogravimetric study of the pyrolysis of scrap tyres. Fuel 1999;78:1575–81. doi:10.1016/S0016-2361(99)00087-3.
[24] Lou JC, Lee GF, Chen KS. Incineration of styrene–butadiene rubber: the influence of heating rate and oxygen content on gas products formation. J Hazard Mater 1998;58:165–78. doi:10.1016/S0304-3894(97)00129-5.
[25] Wan H, Duan F, Han Y, Chyang C, Chen H, Tso J. Characteristics of Fluidized-Bed Combustion with Intermittent Feeding Using Woodblocks and Rubber. 1. Combustion Behavior. Energy Fuels 2012;26:5569–76. doi:10.1021/ef3008882.
[26] Duan F, Wan H, Han Y, Chyang C, Chen H, Tso J. Characteristics of Fluidized Bed Combustion with Intermittent Feeding Using Woodblocks and Rubber. 2. Pollutant Emissions. Energy Fuels 2012;26:5577–82. doi:10.1021/ef300889h.
[27] Ahmed R, Klundert A van de, Lardinois I. Rubber waste: options for small-scale resource recovery. Gouda, the Netherlands; Leiden: WASTE ; Technology Transfer for Development; 1996.
[28] Palotás ÁB, Szemmelvesisz T, Winkler-Sátor L, Koós T, Koncz J, Bánhidi O, et al. Komplex Investigation of Alternative Fuels. Uni-Flexys Co.; 2013.

## Figure captions

**Fig. 1.** Typical samples of the analysed materials.

**Fig. 2.** The programmable oven with rubber sample and thermocouple.

**Fig. 3.** The configuration of the mid-scale FBC test rig.

**Fig. 4.** The fragmentation of a stuck up hose.

**Fig. 5.** TG and DTG curves of hose sample in argon atmosphere.

**Fig. 6.** The DTG curve of a hose sample and TG/MS ion profiles monitored for (a) $H_2O$ (*m/z* 18), $SO_2$ (*m/z* 64), alkyl (*m/z* 43), and alkenyl (*m/z* 69) fragments; (b) butadiene (*m/z* 54), butene (*m/z* 41, 56), and isoprene (*m/z* 67, 68).

**Fig. 7.** TG and DTG curves of a sprue sample in argon atmosphere.

**Fig. 8.** The DTG curve of a sprue sample and TG/MS ion profiles monitored for butadiene (*m/z* 54), isoprene (*m/z* 67, 68), toluyl fragment (*m/z* 91), acrylonitrile, and alkadienyl fragment (*m/z* 53).

**Fig. 9.** The pyrogram of hoses at 550 °C (a), two pyrograms of successive pyrolysis at 350 °C (b) followed by a pyrolysis at 550 °C (c). The identification of the peaks is given in Table 3.

**Fig. 10.** The pyrogram of sprues at 550 °C (a), two pyrograms of successive pyrolysis at 300 °C (b) followed by a pyrolysis at 550 °C (c). The identification of the peaks is given in Table 4.

**Fig. 11.** The measured CO concentration while dropping rubber particles one by one into the BFBC reactor.

**Table 1.**
Properties of the test materials [28].

| Test material: | | Hoses | Sprues |
|---|---|---|---|
| Moisture | % (wt, a.r.) | 0.59 | 0.52 |
| Volatiles | % (wt, d.b.) | 47.39 | 53.50 |
| Ash | % (wt, d.b.) | 15.71 | 19.50 |
| C | % (wt, d.b.) | 74.23 | 68.61 |
| H | % (wt, d.b.) | 6.59 | 6.95 |
| N | % (wt, d.b.) | 0.29 | 1.78 |
| S | % (wt, d.b.) | 0.36 | 0.61 |
| O | % (wt, d.b.) | 2.82 | 2.55 |
| HHV | MJ/kg (d.b.) | 32.24 | 31.15 |

a.r.: as received
d.b.: dry basis

**Table 2.**
Mass loss data of hose and sprue samples in inert atmosphere.

| Sample | Initial mass (mg) | Temperature range (°C) | Temperature of $DTG_{max}$ (°C) | Mass loss (%) |
|---|---|---|---|---|
| Hoses | 0.985 | 50-150 | 100 | 0.5 |
| | | 150-390 | 310 | 28.7 |
| | | 390-540 | 471 | 29.8 |
| | | 540-1000 | 590 | 3.4 |
| Sprues | 0.959 | 50-130 | 100 | 0.5 |
| | | 130-310 | 225 | 13.0 |
| | | 310-530 | 466 | 49.9 |
| | | 530-1000 | 570 | 2.2 |

**Table 3.**
Pyrolysis products of hoses and GC/MS total ion peak areas [(counts/mg polymer) ×$10^{-5}$].

| GC peak number[a] | Retention time (min) | Compound name | Peak area | | |
|---|---|---|---|---|---|
| | | | pyrolysis at 550 °C | successive pyrolysis at 350 °C | at 550 °C |
| 1 | 2.4 | $CO_2$, ethene, and propene | 691 | 47 | 505 |
| 2 | 2.5 | $SO_2$, isobutene, 1,3-butadiene and HCl | 658 | 1397 | 222 |
| 3 | 2.6 | $H_2O$ and 1-pentene | 126 | | 73 |
| 4 | 2.8 | isoprene | 280 | | 91 |
| 5 | 2.9 | 1-hexene | 186 | | 103 |
| 6 | 3.5 | methylcyclopentene and methylcyclopentadiene | 302 | | 92 |
| 7 | 3.8 | 1-heptene and 1,3-cyclohexadiene | 627 | 36 | 137 |
| 8 | 3.9 | benzene | 257 | 43 | 55 |
| 9 | 5.6 | 1-octene | 234 | 28 | 64 |
| 10 | 5.9 | toluene | 178 | | 91 |
| 11 | 7.7 | 1-nonene | 271 | 37 | 64 |
| 12 | 8.7 | dimethylbenzene | 83 | | 35 |
| 13 | 8.9 | styrene | 91 | | 30 |
| 14 | 9.7 | 1-decene | 87 | | 54 |
| 15 | 9.8 | 1-chloroheptane | 184 | 422 | 9 |
| 16 | 10.5 | methylstyrene | 64 | 57 | 14 |
| 17 | 11.1 | 1-heptanol | 127 | 94 | |
| 18 | 11.5 | 1-propenylbenzene and 1-undecene | 146 | | 66 |
| 19 | 11.6 | 1-chlorooctane | 120 | 297 | |
| 20 | 11.9 | indene | 68 | | 31 |
| 21 | 12.7 | 1-octanol | 97 | 69 | |
| 22 | 13.3 | 1-chlorononane | 171 | 389 | |
| 23 | 13.8 | 1-methyl-1H-indene | 61 | | 25 |
| 24 | 14.2 | 1-nonanol | 103 | 106 | |
| 25 | 14.4 | naphthalene | 42 | | 19 |
| 26 | 14.5 | 1-tridecene | 70 | | 46 |
| 27 | 27.6 | 1,2,4-benzenetricarboxylic acid, 1,2-anhydride heptyl ester[a] | 494 | 503 | 38 |
| 28 | 27.7 | hexacosane | 73 | 91 | 24 |
| 29 | 28.4 | 1,2,4-benzenetricarboxylic acid, 1,2-anhydride octyl ester[a] | 283 | 314 | 37 |
| 30 | 28.5 | heptacosane | 104 | 127 | 45 |
| 31 | 29.3 | 1,2,4-benzenetricarboxylic acid, 1,2-anhydride nonyl ester[a] and octacosane | 358 | 456 | 94 |
| 32 | 29.9 | aromatic compound[a] (M: 287) | 280 | 230 | 83 |
| | | sum | 6914 | 4742 | 2146 |

[a] Tentatively identified on the basis of mass spectra.

**Table 4.**
Pyrolysis products of sprues and GC/MS total ion peak areas [(counts/mg polymer) ×$10^{-5}$].

| GC peak number | Retention time (min) | Compound name | Peak area | | |
|---|---|---|---|---|---|
| | | | pyrolysis at 550 °C | successive pyrolysis at 300 °C | at 550 °C |
| 1 | 2.4 | $CO_2$ and propene | 791 | | 844 |
| 2 | 2.5 | isobutene, 1,3-butadiene and $H_2O$ | 1830 | | 792 |
| 3 | 2.8 | isoprene | 360 | | 205 |
| 4 | 3.2 | 2-propenenitrile (acrylonitrile) | 261 | | 127 |
| 5 | 3.8 | methyl-1,3-cyclopentadiene and 2-butenenitrile | 366 | | 221 |
| 6 | 4.0 | benzene | 318 | | 206 |
| 7 | 5.9 | toluene | 317 | | 209 |
| 8 | 6.8 | 4-vinylcyclohexene | 370 | | 132 |
| 9 | 8.0 | ethylbenzene | 106 | | 70 |
| 10 | 8.1 | dimethylbenzene | 107 | | 95 |
| 11 | 8.7 | dimethylbenzene | 191 | | 114 |
| 12 | 8.9 | styrene | 120 | | 68 |
| 13 | 9.8 | propylbenzene | 109 | | 49 |
| 14 | 10.7 | 2,4-hexadienenitrile and ethyl-methylbenzene | 112 | | 70 |
| 15 | 11.5 | 1-propenylbenzene | 113 | | 72 |
| 16 | 11.9 | indene | 106 | | 65 |
| 17 | 12.0 | benzonitrile | 117 | | 60 |
| 18 | 12.7 | 4-cyanocyclohexene | 129 | | 78 |
| 19 | 13.5 | 2,3-dihydroindole | 107 | | 82 |
| 20 | 13.8 | methyl-1H-indene and methylbenzonitrile | 120 | | 93 |
| 21 | 14.2 | tetrahydroquinoline and 2-ethyl-hexanoic acid | 143 | | 150 |
| 22 | 15.5 | benzothiazole | 326 | | 85 |
| 23 | 16.3 | 2-methylnaphthalene | 130 | | 91 |
| 24 | 16.7 | multi-component peak | 115 | | 42 |
| 25 | 16.8 | alyphatic glycol ester[a] | 76 | | |
| 26 | 17.2 | multi-component peak | 135 | | 32 |
| 27 | 18.0 | 2,3-dimethylnaphthalene and aromatic N-containing compound | 117 | | 58 |
| 28 | 18.3 | dimethylquinoline | 122 | | 38 |
| 29 | 18.5 | 1,2-dihydro-2,2,4-trimethylquinoline | 71 | 90 | 20 |
| 30 | 20.4 | alyphatic glycol ester[a] | 298 | | |
| 31 | 25.1 | octadencennitrile | 321 | 230 | |
| 32 | 26.1 | $N^1$-isopropyl-$N^4$-phenylbenzene-1,4-diamine[a] | 403 | 523 | |
| 33 | 26.6 | hexadecanamide | 83 | 162 | |
| 34 | 28.2 | 9-octadecenamide | 748 | 946 | |
| 35 | 28.3 | tri(ethylene glycol) bis(2-ethylhexanoate) | 9253 | 12449 | 1345 |
| 36 | 29.0 | bis(2-ethylhexyl)phthalate | 104 | 190 | |
| 37 | 32.4 | aromatic compound (M=330) | 368 | 178 | 91 |
| | | sum | 18864 | 14766 | 5607 |

[a] Tentatively identified on the basis of mass spectra.


Fig. 1. Typical samples of the analysed materials.

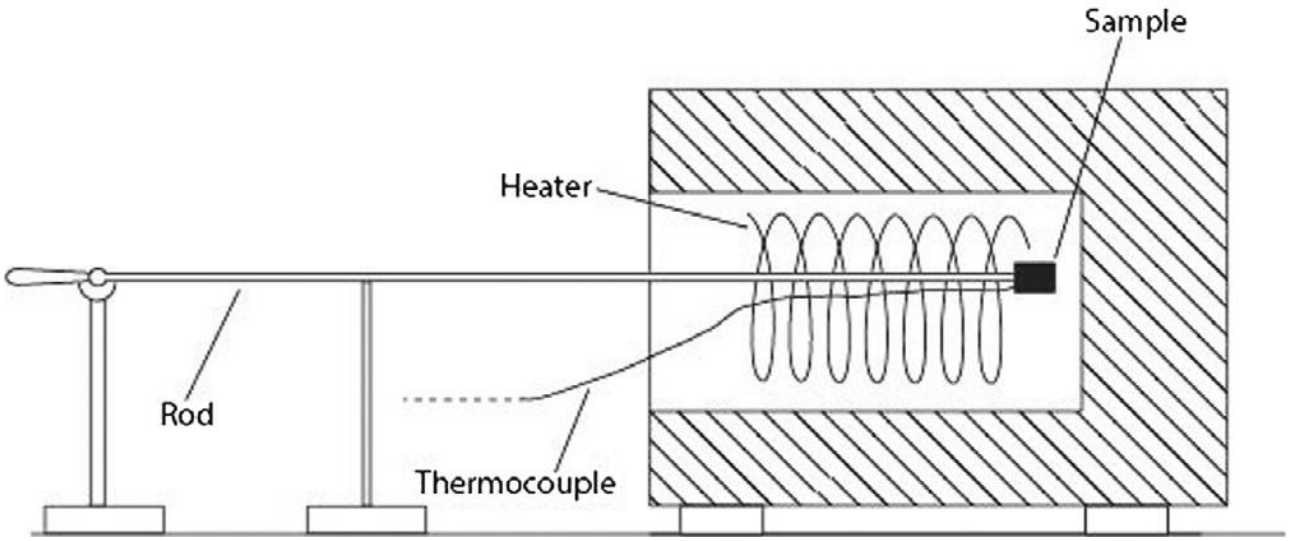


Fig. 2. The programmable oven with rubber sample and thermocouple.

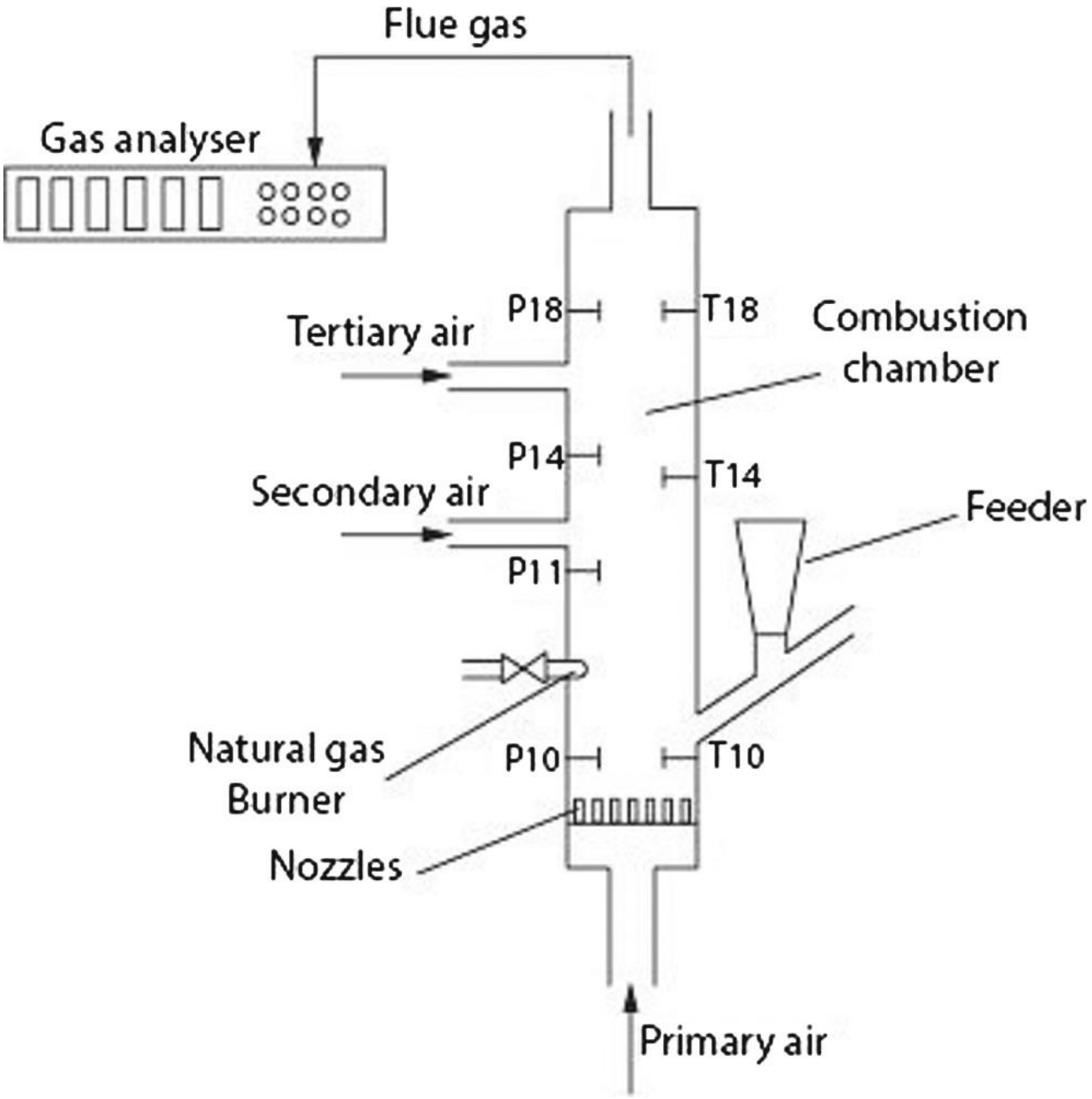


Fig. 3. The configuration of the mid-scale FBC test rig.

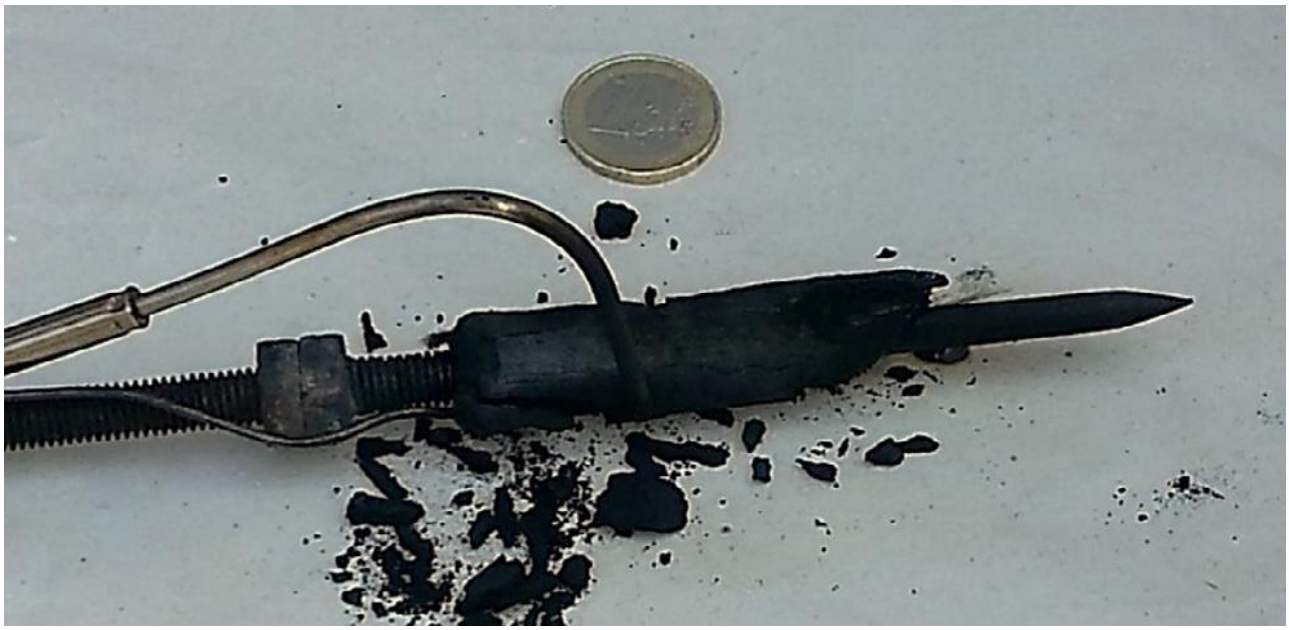

Fig. 4. The fragmentation of a stuck up hose.

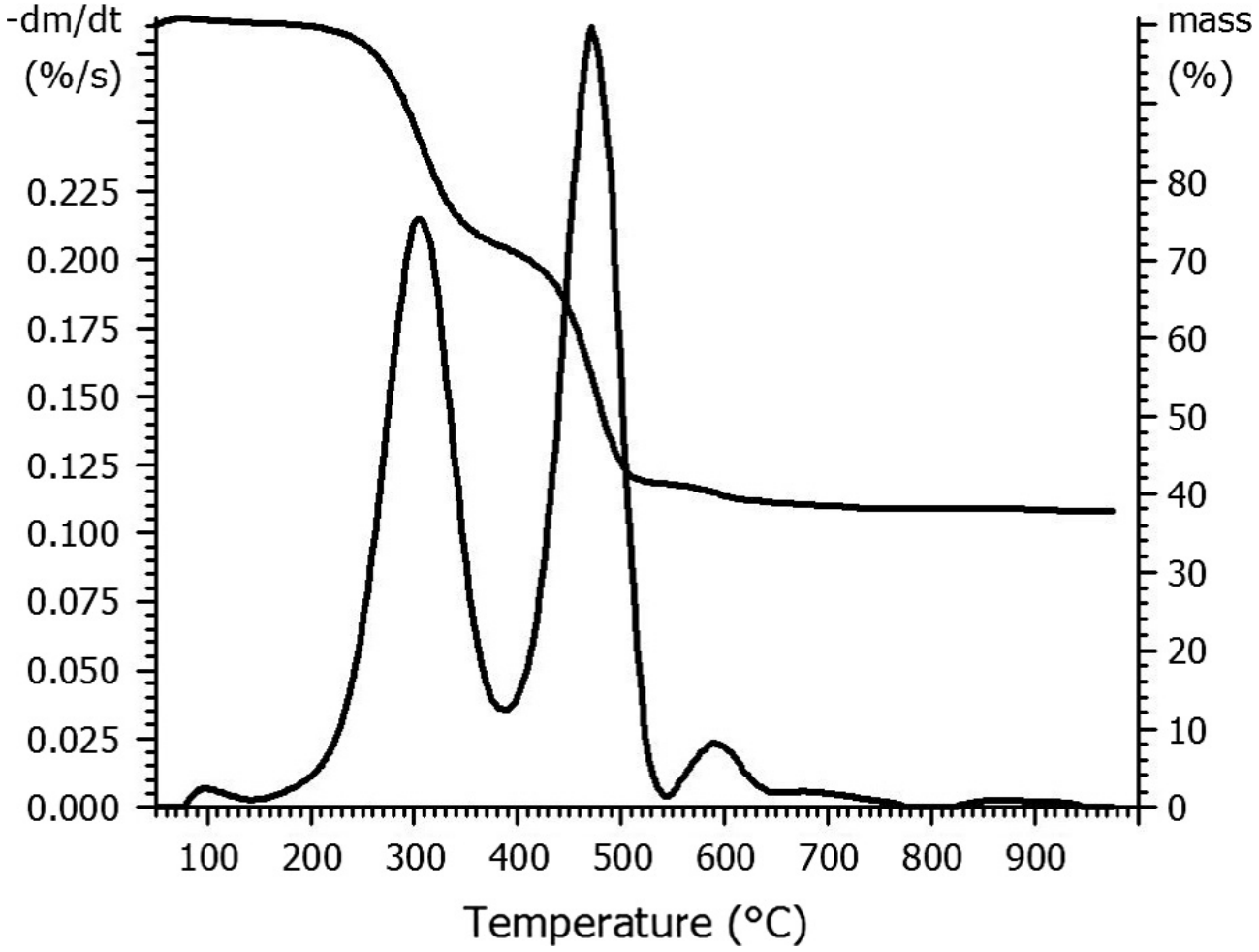


Fig. 5. TG and DTG curves of hose sample in argon atmosphere.

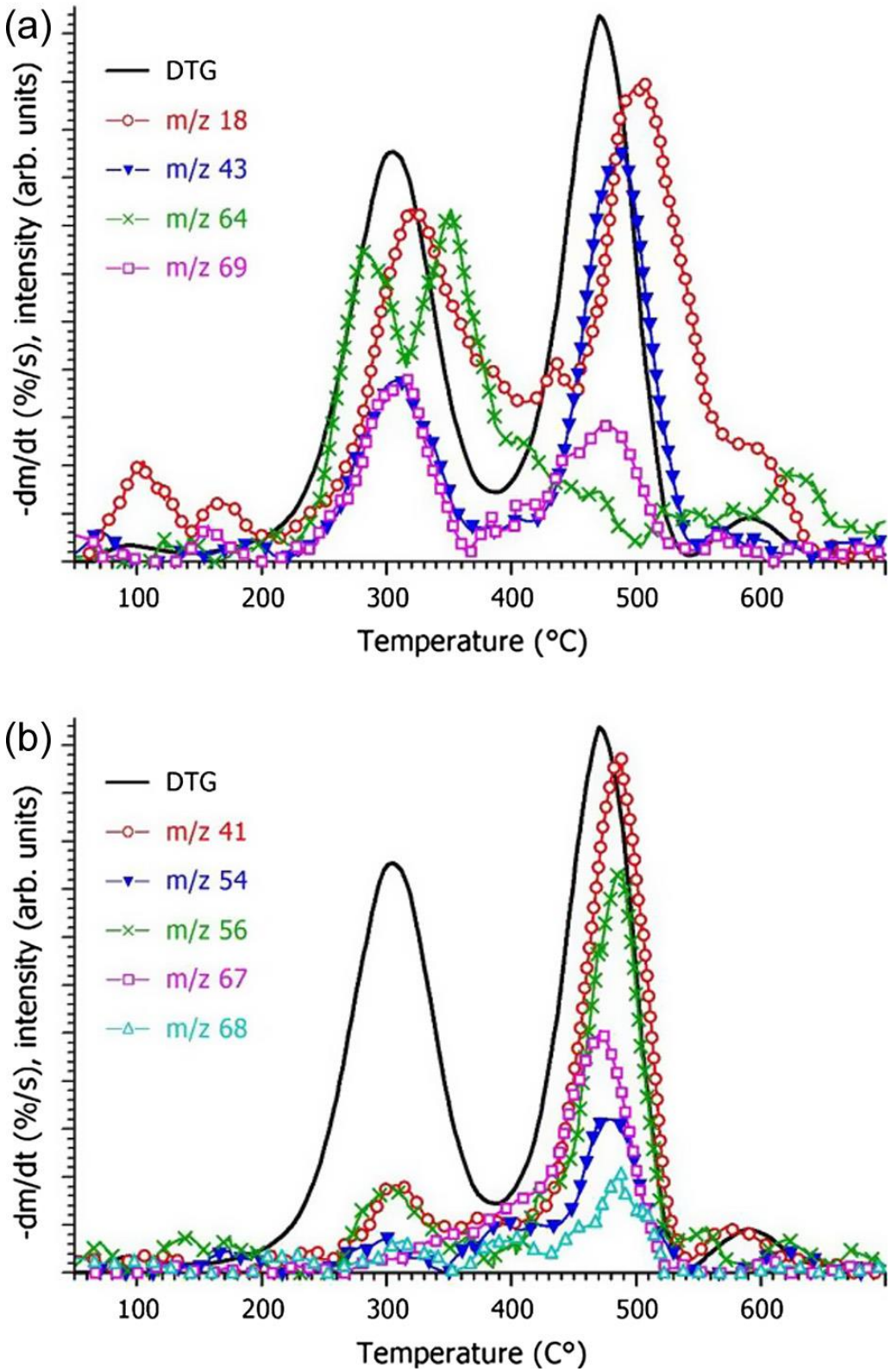


Fig. 6. The DTG curve of a hose sample and TG/MS ion profiles monitored for (a) $H_2O$ (m/z 18), $SO_2$ (m/z 64), alkyl (m/z 43), and alkenyl (m/z 69) fragments; (b) butadiene (m/z 54), butene (m/z 41, 56), and isoprene (m/z 67, 68).

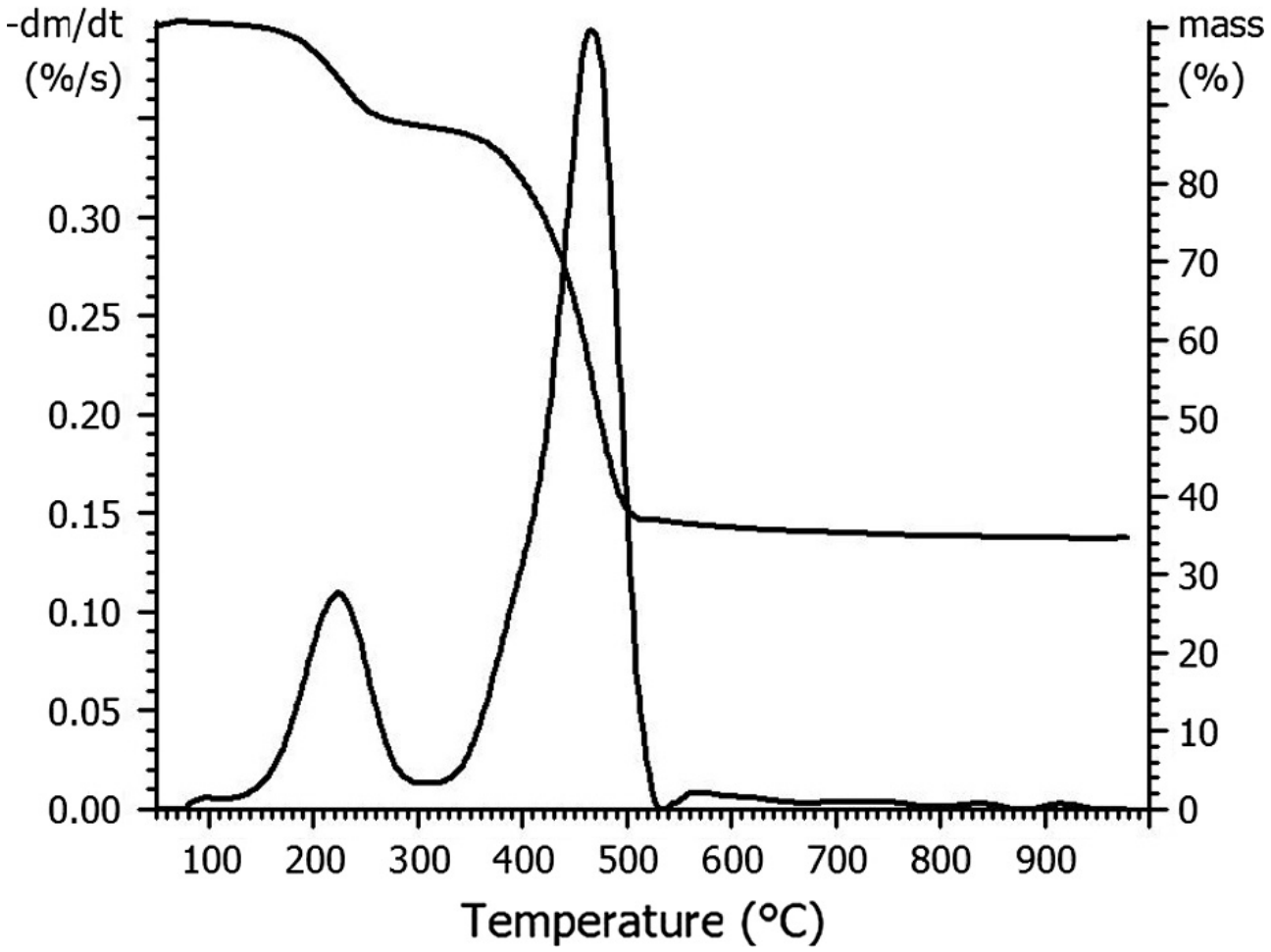


Fig. 7. TG and DTG curves of a sprue sample in argon atmosphere.

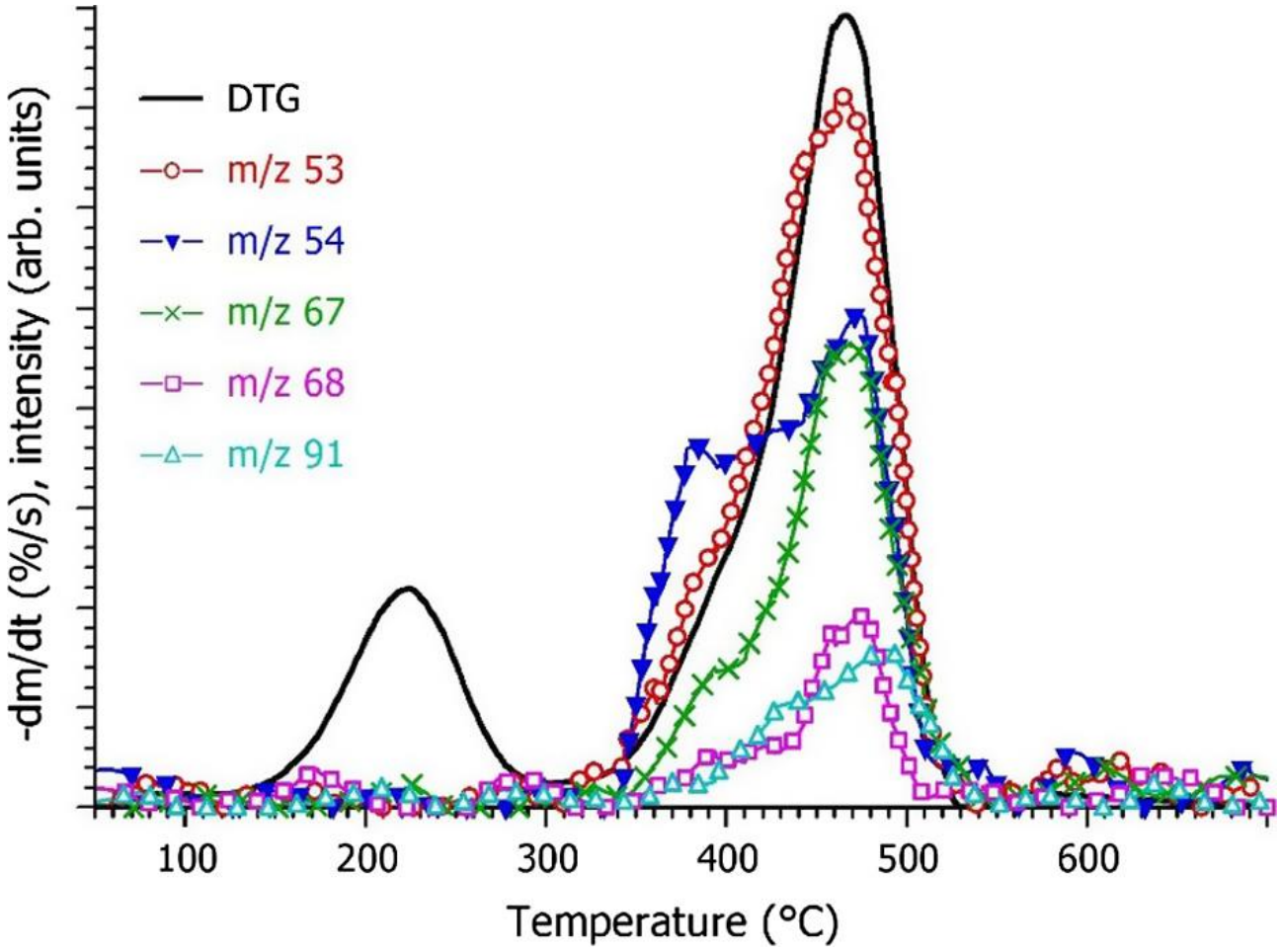


Fig. 8. The DTG curve of a sprue sample and TG/MS ion profiles monitored for butadiene (m/z 54), isoprene (m/z 67, 68), toluyl fragment (m/z 91), acrylonitrile, and alkadienyl fragment (m/z 53).

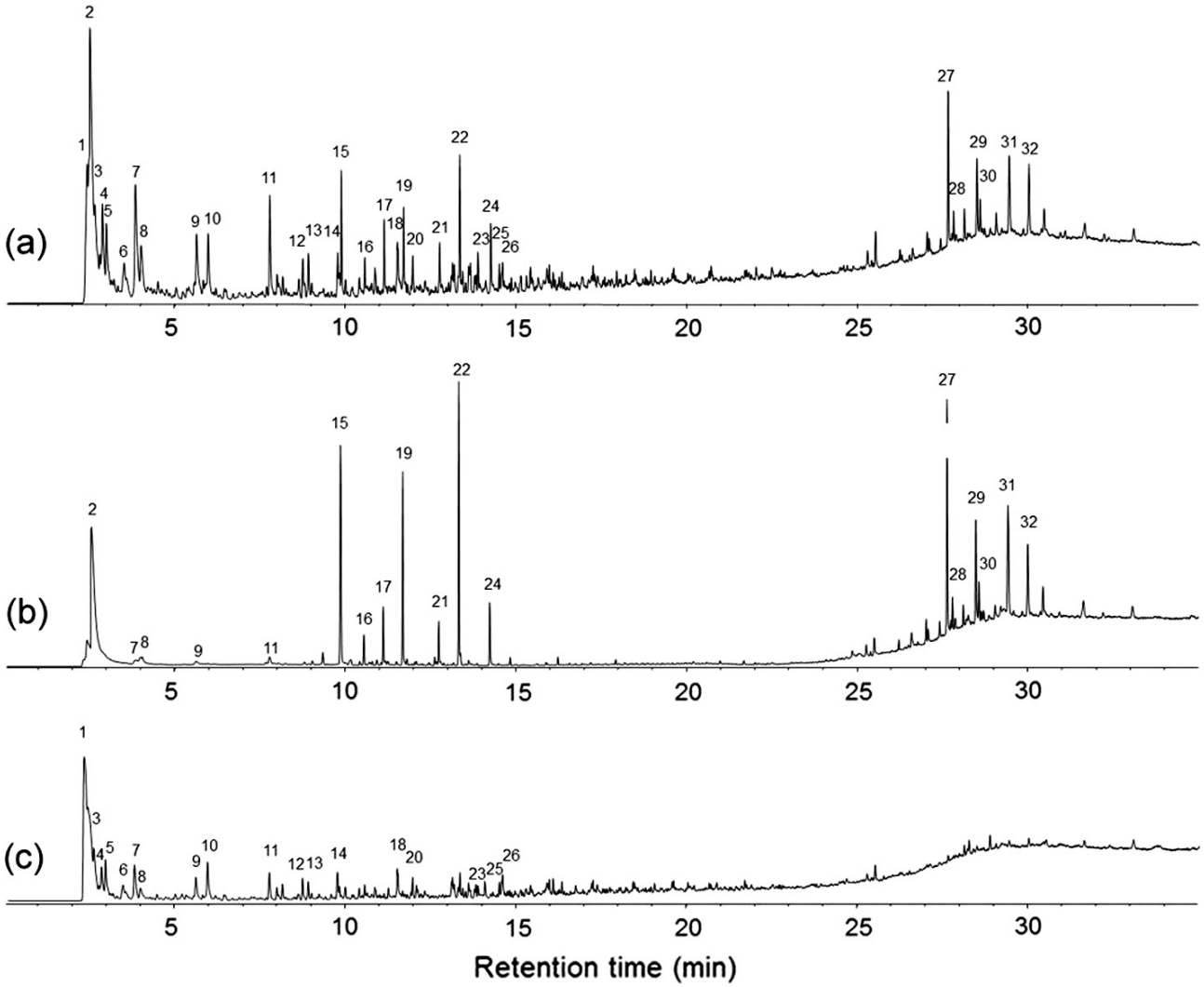


Fig. 9. The pyrogram of hoses at 550 °C (a), two pyrograms of successive pyrolysis at 350 °C (b) followed by a pyrolysis at 550 °C (c). The identification of the peaks is given in Table 3.

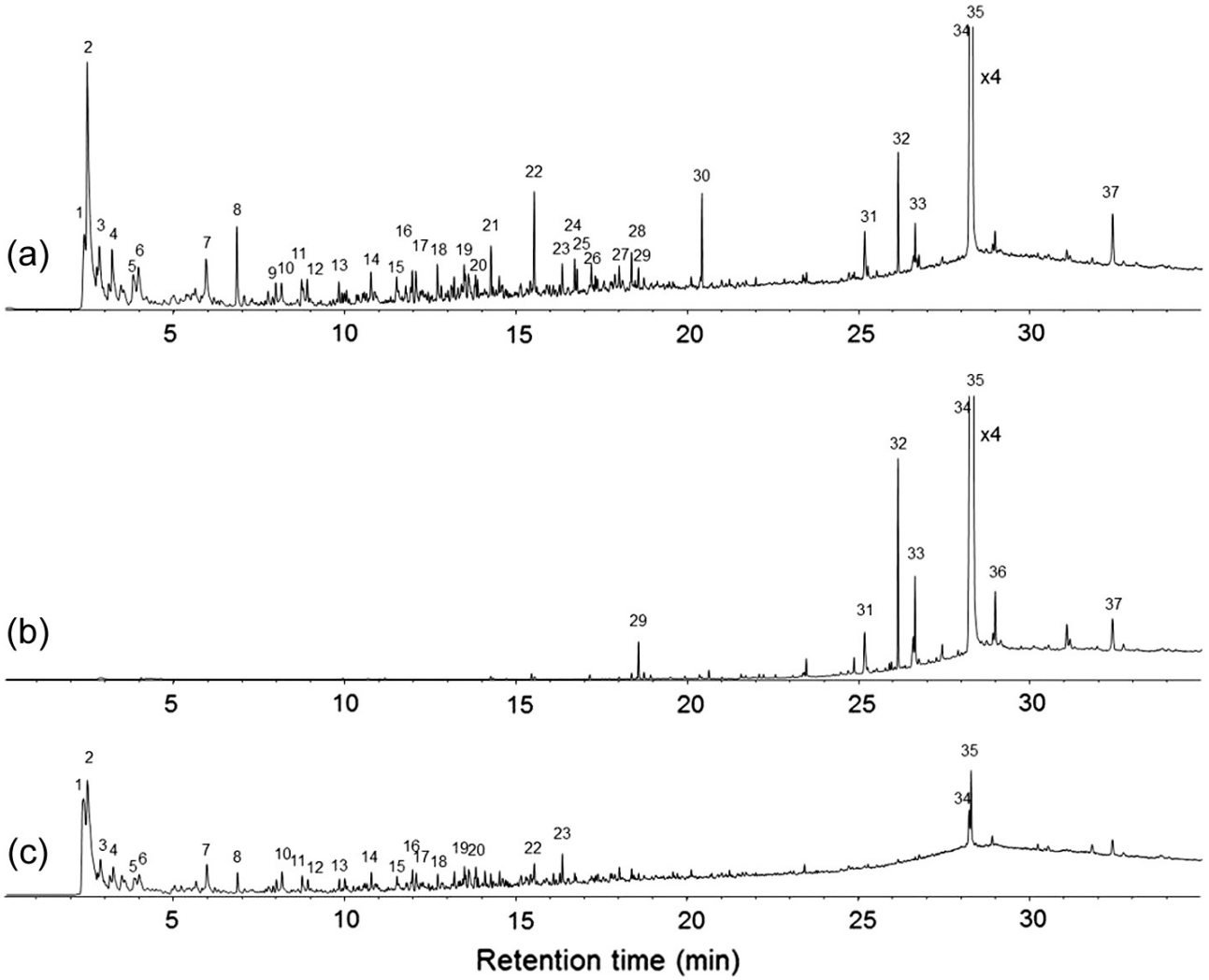


Fig. 10. The pyrogram of sprues at 550 °C (a), two pyrograms of successive pyrolysis at 300 °C (b) followed by a pyrolysis at 550 °C (c). The identification of the peaks is given in Table 4.

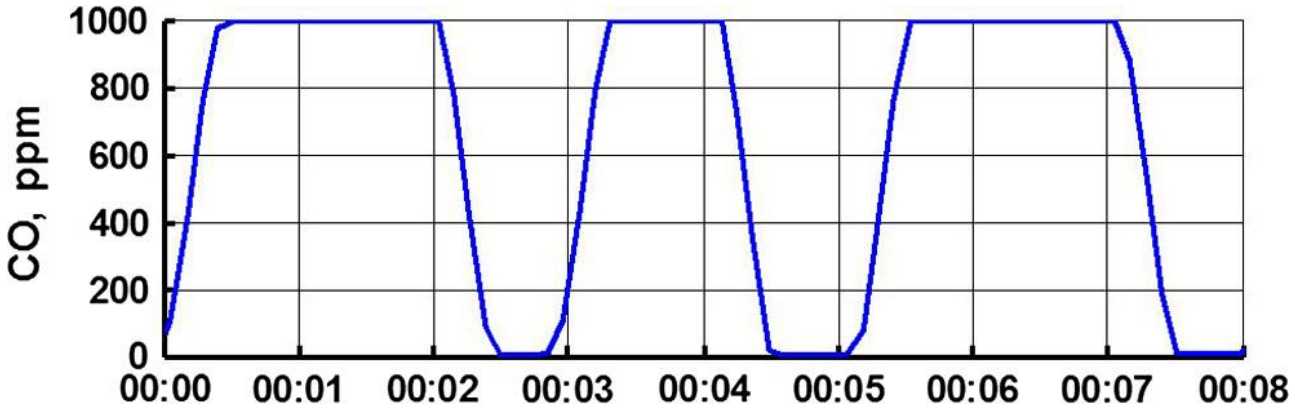


Fig. 11. The measured CO concentration while dropping rubber particles one by one into the BFBC reactor.